

Evidence for deceleration in the radio jets of GRS 1915+105?

J.C.A. Miller-Jones,^{1*} M.P. Rupen,² R.P. Fender,^{3,1} A. Rushton,⁴ G.G. Pooley,⁵ and R.E. Spencer.⁴

¹*Astronomical Institute ‘Anton Pannekoek’, University of Amsterdam, Kruislaan 403, 1098 SJ, Amsterdam, The Netherlands*

²*NRAO, Array Operations Center, 1003 Lopezville Road, Socorro, NM 87801, U.S.A.*

³*School of Physics and Astronomy, University of Southampton, Highfield, Southampton, SO17 1BJ*

⁴*Jodrell Bank Observatory, The University of Manchester, Macclesfield, Cheshire, SK11 9DL*

⁵*Astrophysics, Cavendish Laboratory, J. J. Thomson Avenue, Cambridge CB3 0HE*

Accepted xxxxxxxx. Received xxxxxxxx; in original form xxxxxxxx

ABSTRACT

There is currently a clear discrepancy in the proper motions measured on different angular scales in the approaching radio jets of the black hole X-ray binary GRS 1915+105. Lower velocities were measured with the Very Large Array (VLA) prior to 1996 than were subsequently found from higher-resolution observations made with the Very Long Baseline Array and the Multi-Element Radio Linked Interferometer Network. We initiated an observing campaign to use all three arrays to attempt to track the motion of the jet knots from the 2006 February outburst of the source, giving us unprecedented simultaneous coverage of all angular scales, from milliarcsecond scales out to arcsecond scales. The derived proper motion, which was dominated by the VLA measurements, was found to be 17.0 mas d^{-1} , demonstrating that there has been no significant permanent change in the properties of the jets since 1994. We find no conclusive evidence for deceleration of the jet knots, unless this occurs within 70 mas of the core. We discuss possible causes for the varying proper motions recorded in the literature.

Key words: ISM: jets and outflows – stars: winds, outflows – radio continuum:stars – stars:individual:GRS1915+105 – stars:variables – X-rays: binaries

1 INTRODUCTION

Since they were first observed by Mirabel & Rodríguez (1994), the radio jets in the black hole X-ray binary GRS 1915+105 have been the focus of intensive study. The ejecta have been observed at milliarcsecond scales with the Very Long Baseline Array (VLBA) (Dhawan et al. 2000) and the Multi-Element Radio Linked Interferometer Network (MERLIN) (Fender et al. 1999; Miller-Jones et al. 2005), and at arcsecond scales with the Very Large Array (VLA) (Mirabel & Rodríguez 1994; Rodríguez & Mirabel 1999). Rodríguez & Mirabel (1998) and Kaiser et al. (2004) have also searched on arcminute scales for potential impact sites of the jets on the interstellar medium, although at present the evidence is inconclusive.

The proper motions initially measured by Mirabel & Rodríguez with the VLA were $\mu_{\text{app}} = 17.6 \pm 0.4 \text{ mas d}^{-1}$ for the approaching (southeastern) jet and $\mu_{\text{rec}} = 9.0 \pm 0.1 \text{ mas d}^{-1}$ for the receding (north-

western) counterjet. Rodríguez & Mirabel (1999) used the VLA to measure proper motions for other ejection events, and found fairly consistent values, with no evidence for deceleration of the jets, which were in all cases found to move ballistically outwards from the core. However, MERLIN observations of a 1997 ejection event (Fender et al. 1999) measured a significantly higher set of proper motions, $\mu_{\text{app}} = 23.6 \pm 0.5 \text{ mas d}^{-1}$ and $\mu_{\text{rec}} = 10.0 \pm 0.5 \text{ mas d}^{-1}$, albeit on smaller angular scales. Again, the jet knots were observed to move ballistically. Such high proper motions were also confirmed by VLBA observations (Dhawan et al. 2000) and further MERLIN observations (Miller-Jones et al. 2005). In no case was there ever any evidence for deceleration. Fig. 1 shows all the published proper motions for the jets in this system as a function of time, and highlights the stark discrepancy between observations prior to 1997 made with the VLA and those made later with higher-resolution arrays. The actual data are listed in Table 1.

Several possibilities have been put forward to explain this apparent discrepancy in the motion of the jet knots between milliarcsecond angular scales, as measured with MER-

* email: jmiller@science.uva.nl

Table 1. Published proper motions for the jets in GRS 1915+105.

Outburst date	μ_{app} (mas d $^{-1}$)	μ_{rec} (mas d $^{-1}$)	Instrument	Reference
29 Jan 1994	17 ± 2		VLA	Rodríguez & Mirabel (1999)
19 Feb 1994	17.7 ± 0.4	7 ± 2	VLA	Rodríguez & Mirabel (1999)
19 Mar 1994	17.6 ± 0.4	9.0 ± 0.1	VLA	Mirabel & Rodríguez (1994)
21 Apr 1994	16.0 ± 0.7	8.8 ± 1.0	VLA	Rodríguez & Mirabel (1999)
10 Aug 1995	11 ± 2^a	9 ± 2^a	VLA	Rodríguez & Mirabel (1999)
28 Oct 1997	22.1 ± 1.9^b		VLBA	Dhawan et al. (2000)
29 Apr 1998	22.3 ± 1.6^b		VLBA	Dhawan et al. (2000)
01 Nov 1997	23.6 ± 0.5	10.0 ± 0.5	MERLIN	Fender et al. (1999)
04 Nov 1997	23.6 ± 0.5		MERLIN	Fender et al. (1999)
06 Nov 1997	23.6 ± 0.5		MERLIN	Fender et al. (1999)
21 Mar 2001	20.3 ± 0.7^c	12.4 ± 0.5^c	MERLIN	Miller-Jones et al. (2005)
27 Mar 2001	24.4 ± 1.1^c		MERLIN	Miller-Jones et al. (2005)
31 Mar 2001	25.1 ± 0.7^c		MERLIN	Miller-Jones et al. (2005)
16 Jul 2001	23.2 ± 0.9^c	12.1 ± 2.0^c	MERLIN	Miller-Jones et al. (2005)

^a Since this proper motion was based on only a single pair of individual condensations, it was considered unreliable.

^b Converted from the proper motions per hour quoted by Dhawan et al. (2000).

^c It was found that the positional uncertainties in Miller-Jones et al. (2005) had been overestimated, so the fits to the data were redone using the revised error bars to give the proper motions quoted here, with associated uncertainties.

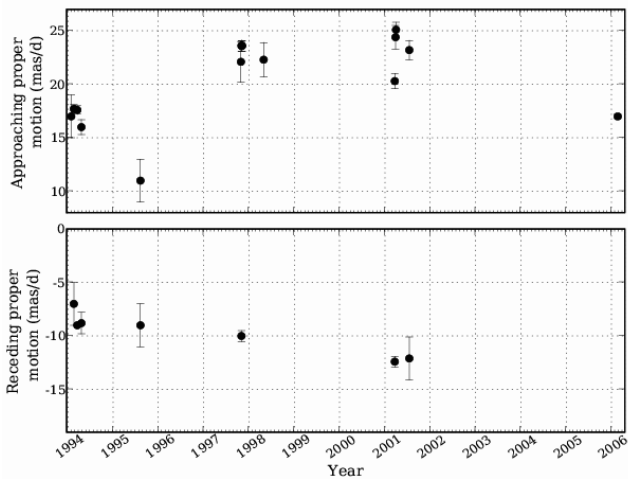


Figure 1. Measured proper motions in GRS 1915+105, as a function of time. The August 1995 point was made from only a single pair of individual condensations, so was considered unreliable (Rodríguez & Mirabel 1999).

LIN and the VLBA, and those seen on arcsecond scales with the VLA. Fender et al. (1999) found that the discrepancy could not be explained away by a simple change in the angle to the line of sight of an otherwise physically identical jet (i.e. ruling out precession). They suggested two possible explanations; either the jet velocities were intrinsically different, or resolution effects were at work between the two arrays. This latter would lead to a blending of components, and would explain the proper motion discrepancy if there was a sequence of ejecta which decreased sequentially more rapidly in flux density with increasing distance from the core (such that each ejected knot decayed more slowly than its predecessors). This effect was originally highlighted by Hjellming & Rupen (1995) for the case of GRO J1655–40.

Observing the same outburst sequence with both the VLBA and VLA, they found a similar reduction in the fitted proper motion from 54 to 40 mas d $^{-1}$ on moving from VLBA to VLA angular scales. They suggested that a combination of the flux density fading with time and spatial averaging of underlying structures led to the discrepancy.

A further possibility is that the knots could be decelerating as they moved outwards (which would imply that they could not be highly relativistic after the deceleration, since the Lorentz factor Γ must be of order 2 to see discernible changes in the proper motion), although the ballistic motions of the observed knots would tend to argue against this. Alternatively, as pointed out by Miller-Jones et al. (2005), there could have been an intrinsic change in the system between the time when the VLA observations were taken (all between 1994 and 1995) and the time when the higher-resolution observations were made (between 1997 and 2001). Since the source was not detected until 1992 (Castro-Tirado et al. 1992), despite the existing X-ray satellites prior to that time having the sensitivity to detect it, the system might only have emerged from quiescence at that time. Indeed, Truss & Done (2006) suggested that the system has been in a continuous outburst phase since 1992, and may soon switch off again, moving back into quiescence. In this case, the powerful jets might since 1992 have evacuated a cavity through which the ejecta could propagate, such that they could coast for longer during later outbursts, giving rise to the higher proper motions measured with the VLBA and MERLIN. As suggested by Heinz (2002), this would explain the location of the system within a region of very low ISM density, although in that case the jet would have needed to have been active for a timescale of order 10^3 years, rather than only since 1992.

To try to discern the cause of this proper motion discrepancy, we proposed to track the motion of the ejecta in GRS 1915+105 over all available angular scales, using the VLBA, MERLIN and also the VLA. In Section 2, we detail

our observations, in Section 3 we discuss our results, and in Section 4 we draw our conclusions.

2 OBSERVATIONS AND DATA REDUCTION

We triggered our Target of Opportunity proposal (Miller-Jones et al. 2006) after being alerted to a radio flare in the system by the RATAN-600 monitoring programme (S. Trushkin, private communication). The *Rossi X-ray Timing Explorer (RXTE)* All Sky Monitor (ASM) data showed that this coincided with a significant X-ray flare, giving us confidence that an ejection event was underway. We obtained four epochs of VLBA observations, three of MERLIN observations, and quasi-weekly monitoring with the VLA until the end of its A-configuration trimester. A montage of all the observations made during the initial period when all three arrays were taking data is shown in Fig. 2.

2.1 VLBA observations

The VLBA observations were made in parallel at two different frequencies, 8.42 and 2.27 GHz. Observations were taken using dual polarisation, 2-bit sampling, with sixteen 500-kHz channels giving a total bandwidth of 8 MHz at each frequency.

GRS 1915+105 is scatter-broadened, with a scattering size of 1.9 ± 0.1 mas at 8.4 GHz, scaling as λ^2 (Dhawan et al. 2000). This corresponds to a scattering size of 25.6 mas for the longer wavelength observations at 2.3 GHz. We were therefore unable to make use of the full resolution of the array, and were forced to discard the longest baselines (most affected by the scattering) before imaging. We imaged with a robust weighting parameter biased toward natural weighting, applying a Gaussian taper in the uv -plane to down-weight the contributions of the longest remaining baselines.

The integrated flux density of the source did not appear to vary by more than 10–20 per cent during any of the four observing runs, so the images were made with the full timerange available at each epoch (4 h for the first epoch, and 6 h for the other three) to maximise the uv -coverage. With an assumed proper motion of 24 mas d^{-1} (as seen in the previous high-resolution observations), components would move approximately one beamwidth over the course of the observation at 8.4 GHz and half a beamwidth at 2.3 GHz, leading to some smearing of the components in the images. This effect has been investigated by previous authors (e.g. Mioduszewski et al. 2001), and has been shown not to significantly affect the conclusions that can be drawn from such images.

The VLBA measurements are summarised in Table 2, and the images can be seen in Fig. 2. Only in the first of the four epochs was the original southeastern component seen which corresponded to the knot monitored with the VLA (Section 2.3). Its separation of 135.9 ± 0.5 mas at position angle 142.3 ± 0.2 agrees well with that seen at the VLA (see Table 3) on the same day (MJD 53794). Both the core and the ejecta appear slightly elongated, and in both the 8.4 and 2.3 GHz images there appears to be a hint of a receding northwestern component.

By the second epoch (MJD 53798), the southeastern

component has faded and is no longer detectable, although there is evidence that at least two new sets of knots have been ejected. In the 8.4 GHz image, we see both the approaching and receding components, and the core component appears to be marginally elongated, hinting at an even more recent ejection event. The size of the scattering disc at 2.3 GHz prevents us from seeing this structure as clearly at the longer wavelength, although the source is certainly resolved.

Two days later, at MJD 53800, these new components have also faded at 8.4 GHz, and the image shows an unresolved core and a new, resolved southeastern component. At the lower frequency however, the source is clearly resolved, and a component presumably corresponding to the knots from the previous epoch can be seen at an angular separation of 48.9 ± 1.5 mas.

In the last epoch, MJD 53803, we again see an unresolved core and a very weak southeastern component at 8.4 GHz. For the known range of proper motions of the ejecta in this system ($16\text{--}24 \text{ mas d}^{-1}$), the approaching component in this image cannot be related to those seen in the previous two images. No source was detected at 2.3 GHz. For this observing run, we were missing two of the antennas in the southwestern United States (Fort Davies and Pie Town), which removed several of the short baselines in the array. Coupled with the loss of the long baselines to scattering, this rather compromised the uv -coverage, which might explain the non-detection.

2.2 MERLIN observations

Three epochs of MERLIN observations were taken. The observing frequency was 6.0353 GHz with a bandwidth of 14 MHz. At each epoch, in addition to the target source GRS 1915+105, observations were made of the flux and polarisation angle calibrator 3C 286, the point source calibrator OQ 208, and the phase reference source B 1919+086, 2.8 away from the target source. The observations were made using the five outstations (Cambridge, Defford, Knockin, Darnhall and Tabley) and the Mark 2 antenna at Jodrell Bank.

The MERLIN d-programs were used to perform initial data editing and amplitude calibration, and the data were then imported into the National Radio Astronomy Observatory's (NRAO) ASTRONOMICAL IMAGE PROCESSING SYSTEM (AIPS) software package for further data reduction. The MERLIN pipeline was then used to image and self-calibrate the phase reference source, and apply the derived corrections to the target source, GRS 1915+105, which was subjected to further iterations of phase-only self-calibration.

The first MERLIN epoch caught the start of a flare, seen to begin at 11:10 UT on 2006 March 3 (MJD 53797.465 \pm 0.003). The variable amplitude meant that the last few hours of observation had to be flagged to prevent the violation of the basic assumption of synthesis imaging that the source structure should not change during the observation. Similarly, the second epoch of observation caught the decay of a further flare, dropping from 107 to 20 mJy between 02:30 and 09:00 UT. Nevertheless, imaging that epoch after removing the affected data showed both the core component and a southeastern jet knot at an angular separation of

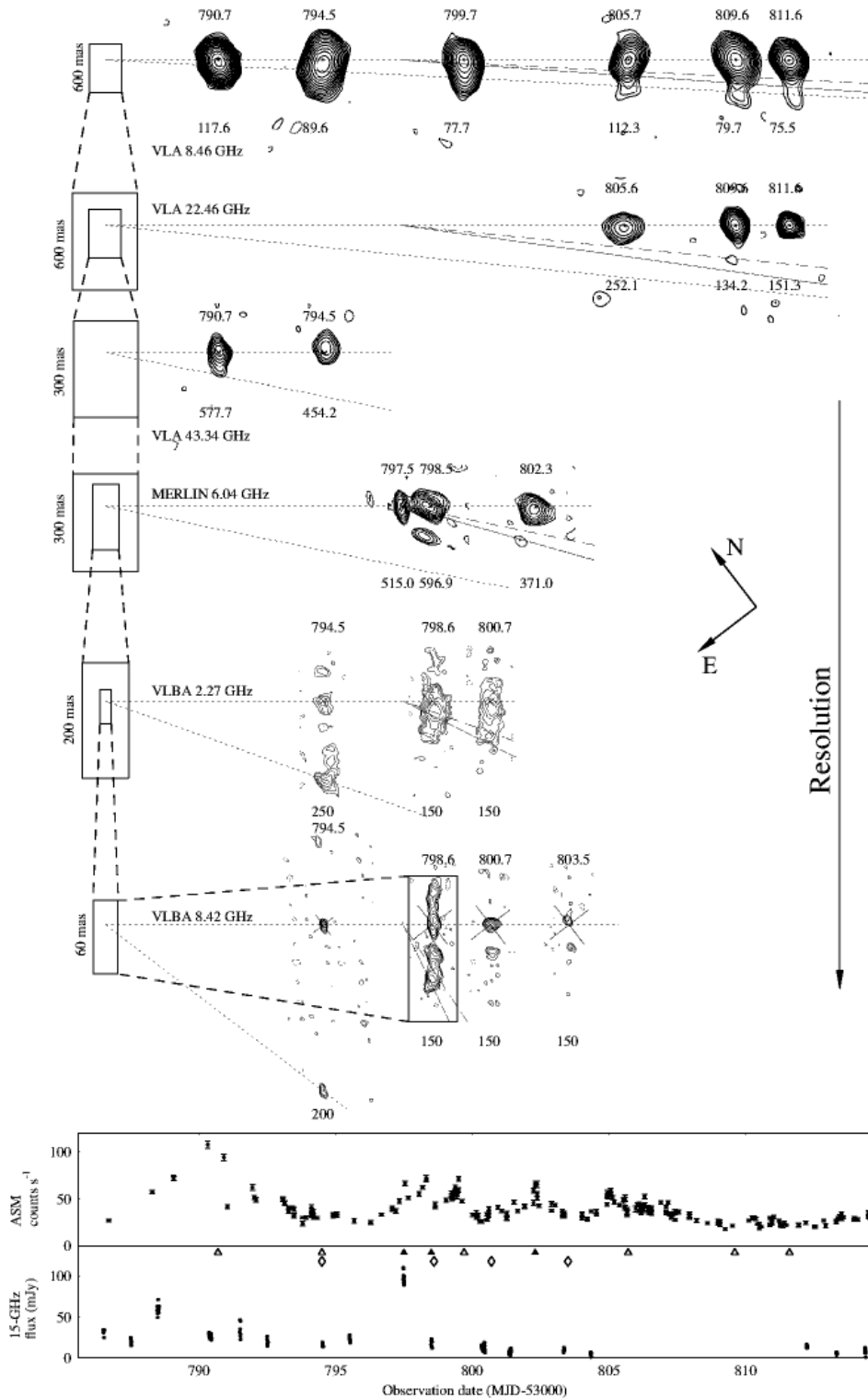


Figure 2. Radio images from our monitoring campaign. Flux densities from the 15-GHz Ryle monitoring programme and the 1.5–12 keV X-ray count rates measured by the *RXTE* ASM are shown in the two bottom plots. Open triangles at the top of the Ryle plot mark the times of the VLA observations, diamonds the VLBA observations, and filled triangles the MERLIN observations. Resolution gets better on moving down the page, showing, in order, VLA 8.46 GHz images (top), VLA 22.46 GHz images, VLA 43.34 GHz images, MERLIN 6.03 GHz images, VLBA 2.27 GHz images, and finally VLBA 8.42 GHz images (bottom; note the different scale for the first epoch). The dates of the observations (MJD – 53000) are shown above each radio image, and the image rms (in $\mu\text{Jy beam}^{-1}$) below. Contours are at levels of $\pm(\sqrt{2})^n$ times the rms level, where $n = 3, 4, 5, \dots$. The predicted position of the VLBA core (V. Dhawan, private communication) is marked by a cross. All images have been rotated anticlockwise by 37.5° . Dotted lines show the core position and the fitted proper motion of 17.0 mas d^{-1} from the initial ejection event, and the dashed and dot-dashed lines show nominal proper motions of 23.6 and 17.0 mas d^{-1} respectively, for an ejection event taking place at the time of the detected MERLIN flare.

Table 2. VLBA observations of GRS 1915+105.

Observation date (MJD)	Frequency (GHz)	Component	Angular Separation (mas)	PA (degs)	Flux density (mJy)
53794.541 ± 0.081	8.4	Core	0	0	8.97 ± 0.56
53794.541 ± 0.081	8.4	SE	135.9 ± 0.5	142.3 ± 0.2	4.44 ± 0.68
53794.541 ± 0.081	8.4	NW	68.2 ± 0.8	-34.0 ± 0.6	1.13 ± 0.20
53794.541 ± 0.081	2.3	Core	0	0	6.21 ± 0.91
53794.541 ± 0.081	2.3	SE1	16.0 ± 1.3	163.1 ± 4.5	5.00 ± 0.44
53794.541 ± 0.081	2.3	SE2	139.6 ± 0.7	141.6 ± 0.3	11.34 ± 1.12
53794.541 ± 0.081	2.3	NW	51.5 ± 2.1	-41.4 ± 2.3	1.94 ± 0.67
53798.564 ± 0.125	8.4	Core	0	0	6.78 ± 0.73
53798.564 ± 0.125	8.4	SE1	12.9 ± 0.3	142.6 ± 1.4	5.61 ± 0.49
53798.564 ± 0.125	8.4	SE2	23.2 ± 0.3	140.7 ± 0.8	6.61 ± 0.52
53798.564 ± 0.125	8.4	NW1	8.2 ± 0.4	-31.8 ± 2.3	3.38 ± 0.42
53798.564 ± 0.125	8.4	NW2	13.3 ± 0.3	-37.9 ± 1.3	2.98 ± 0.34
53800.657 ± 0.124	8.4	Core	0	0	4.04 ± 0.30
53800.657 ± 0.124	8.4	SE	11.5 ± 0.3	145.3 ± 1.4	2.15 ± 0.39
53800.657 ± 0.124	2.3	Core	0	0	8.53 ± 0.87
53800.657 ± 0.124	2.3	SE	48.9 ± 1.5	138.5 ± 1.8	3.38 ± 0.60
53803.525 ± 0.124	8.4	Core	0	0	3.32 ± 0.60
53803.525 ± 0.124	8.4	SE	10.9 ± 0.4	150.7 ± 1.6	2.85 ± 0.58

115.5 ± 3.1 mas. The final epoch appeared to show only an unresolved core. The images are shown in Fig. 2.

2.3 VLA observations

The VLA was in A-configuration, and 1-hour observations were made on a quasi-weekly basis. The main observing frequency was 8.46 GHz, although initially when the source was bright, higher frequencies were also used in an attempt to improve the resolution. As the ejecta moved outwards and faded below detectability at 8.46 GHz, lower frequencies were used in order to take advantage of the assumed steep spectrum ($\nu^{-0.75}$) of the jet knots to aid in their detection.

In all cases, the flux calibrator was 3C 48, and the phase calibrator was J 1924+156, at an angular separation of 5°25 from the target source. The fast switching mode was used at frequencies above 5 GHz in order to reduce the slew time between the secondary calibrator and the target while cycling between the two fast enough to account for tropospheric phase variations. This allowed for diffraction-limited imaging at high frequencies with the long baselines available in A-configuration, in the case that the source was not strong enough for self-calibration to work reliably. Data reduction was performed using standard procedures within AIPS.

2.3.1 The flare of 2006 January

The 15-GHz Ryle Telescope monitoring programme (Pooley & Fender 1997) detected a flare from GRS 1915+105 which peaked at 211 mJy on MJD 53752.6 (2006 January 17). But since the 15-GHz monitoring was not continuous, the start of the flare could have been as early as MJD 53750.6. The source was resolved by the VLA into two components on both MJD 53761 and MJD 53765. The proper motion between these two epochs was $25.4 \pm 0.9 \text{ mas d}^{-1}$. From the fitted positions of the two components in the maps prior to self-calibration, there is

evidence that both the northwestern and the southeastern components moved between the two epochs, the former along position angle $-36.7 \pm 3.4^\circ$ and the latter along $146.5 \pm 2.8^\circ$. This suggests that the proper motion we see is the sum of the proper motions of the approaching and receding components, so that of the approaching component alone is likely to be somewhat lower. These images are shown separately in Fig. 3.

2.3.2 The flare of 2006 February

The main radio flare on which we triggered our multi-resolution observing campaign appeared to peak on MJD 53788.5 (2006 February 22). We tracked one single ejected component for 59 days with the VLA as it moved southeast, out to an angular separation of over 1 arcsec. The full sequence of images is shown in Fig. 4. The ejection event appeared to be one-sided, since only on MJD 53817 do we see any evidence for a receding component.

Tracking the ejected knot over such a long time interval gave extremely good constraints on its proper motion, which we fitted as $17.0 \pm 0.2 \text{ mas d}^{-1}$. This fit (to the VLA proper motions only) is shown in Fig. 5. It is clearly incompatible with the proper motions measured by Fender et al. (1999), and there is no evidence for any deceleration. To verify this, we fitted the angular separations with both a straight-line fit (ballistic motion) and a quadratic fit (corresponding to deceleration), and performed an F-test (e.g. Pfenniger & Revaz 2005). This gave a value $F_{1,10} = 0.81$, implying that the quadratic fit was not significantly better, i.e. there was no significant evidence for any deceleration of the ejecta on the angular scales probed by the VLA.

2.3.3 Flux density decay

Between 8 and about 50 days after the 2006 February ejection event, the flux density of the southeastern component

Table 3. VLA observations of GRS 1915+105.

Observation date (MJD)	Frequency (GHz)	Angular Separation (mas)	PA (degs)	Core flux density (mJy)	SE component flux density (mJy)
53761.72749 ± 0.00272	8.46	190.1 ± 0.9	142.5 ± 0.3	18.34 ± 0.28	41.30 ± 0.27
53761.73860 ± 0.00573	43.34	191.7 ± 5.6	145.8 ± 1.7	23.59 ± 0.93	2.60 ± 1.15
53765.71609 ± 0.00231	8.46	291.5 ± 3.6	144.9 ± 0.7	5.14 ± 0.25	8.91 ± 0.30
53765.72678 ± 0.00571	43.34			1.54 ± 0.39	
53790.68594 ± 0.00145	8.46	68.9 ± 0.6	148.0 ± 0.5	26.85 ± 0.12	24.53 ± 0.12
53790.69282 ± 0.00289	43.34	50.4 ± 2.3	140.8 ± 2.4	18.62 ± 0.65	5.16 ± 0.57
53794.50428 ± 0.00405	8.46	135.9 ± 1.2	147.6 ± 0.5	12.24 ± 0.09	12.09 ± 0.09
53794.51493 ± 0.00405	43.34			3.98 ± 0.53	
53799.65492 ± 0.00318	8.46	209.0 ± 2.6	143.8 ± 0.7	8.55 ± 0.09	3.22 ± 0.09
53805.68200 ± 0.00376	8.46	319.0 ± 19.1	143.8 ± 3.6	11.28 ± 0.15	0.74 ± 0.15
53805.59288 ± 0.00480	22.46			6.26 ± 0.53	
53809.61429 ± 0.00330	8.46	379.0 ± 15.1	147.6 ± 2.0	13.39 ± 0.08	0.65 ± 0.08
53809.62459 ± 0.00480	22.46	217.4 ± 16.0	137.1 ± 4.1	7.24 ± 0.25	0.42 ± 0.15
53811.57042 ± 0.00492	8.46	458.2 ± 27.1	150.7 ± 2.8	12.18 ± 0.14	0.47 ± 0.08
53811.58380 ± 0.00579	22.46			10.02 ± 0.28	
53817.64936 ± 0.01835	8.46	460.0 ± 17.6	146.5 ± 1.9	6.17 ± 0.06	0.29 ± 0.03
53824.58872 ± 0.01823	8.46	685.0 ± 23.6	143.4 ± 1.8	8.26 ± 0.06	0.16 ± 0.03
53831.59398 ± 0.01898	4.86	751.6 ± 33.9	147.4 ± 2.2	3.72 ± 0.09	0.21 ± 0.05
53838.63336 ± 0.01829	8.46	834.9 ± 48.1	138.9 ± 3.3	3.86 ± 0.06	0.09 ± 0.03
53845.57801 ± 0.02037	1.425	1004.8 ± 87.9	152.8 ± 4.2	24.20 ± 0.09	0.57 ± 0.08
53854.62338 ± 0.01991	1.425			14.90 ± 0.10	
53859.62893 ± 0.02766	1.425			167.65 ± 0.30 ^a	

^a In fact the source flux density rose from 135 to 180 mJy during this observing run.

appeared to follow a power-law decay with time (and, since the motion is ballistic, then also with angular separation), $S = S_0(t-t_0)^{-\tau}$, with the exponent fitted as $\tau = 2.70 \pm 0.05$, and where t and t_0 are both measured in days. This is shown in Fig. 6. Where the observations were taken at a lower frequency than 8.4 GHz, the flux densities were extrapolated to give the expected 8.4 GHz flux density, assuming a steep synchrotron spectrum, $S_\nu = S_0(\nu/\nu_0)^{-0.75}$. The derived value of τ is consistent with that of 2.6 ± 0.5 found by Rodríguez & Mirabel (1999) in GRS 1915+105 on angular scales greater than 1 arcsec from the core. In a previous outburst, they found $\tau = 1.3 \pm 0.2$ on angular scales within 1 arcsec, and suggested that there could be a transition from a regime of slowed to free expansion at some distance from the core, as suggested for the case of SS 433 by Hjellming & Johnston (1988). Our observations track the knot out to a distance of ~ 1 arcsec, suggesting that any transition from slowed to free expansion took place much closer to the core during our outburst than in those monitored by Rodríguez & Mirabel (1999). Indeed, if we interpret the low flux density of the first measurement in Fig. 6 as due to an initial phase of slowed expansion, then the transition to free expansion would occur within 135 mas.

Hjellming & Johnston (1988) showed that the flux density decay for a single impulsive ejection, expanding according to a conical jet model, would scale as

$$S \propto (t/t_0)^{-(7p-1)/(6+6\xi)}, \quad (1)$$

where p is the index of the electron energy spectrum, and $\xi = 1$ for slowed expansion and $\xi = 0$ for free expansion. Their derived value of $p = 2.32$ for SS 433 gave indices of 1.27 during the slowed expansion phase and 2.54 dur-

ing free expansion, remarkably consistent with the values found for GRS 1915+105 by Rodríguez & Mirabel (1999) and suggesting a very similar electron energy spectrum in the two sources. Our derived power-law index τ would in this case suggest that we were observing the knot during its freely-expanding phase. In fact, from our fitted value $\tau = 2.70 \pm 0.05$, we can calculate from Equation 1 a corresponding electron index $p = 2.46 \pm 0.04$ and a spectral index $\alpha = -0.73 \pm 0.02$. While not strictly within the error bars, this is broadly consistent with the previously-measured values of 0.8 (Fender et al. 1999) and 0.84 ± 0.03 (Mirabel & Rodríguez 1994), implying that the data can be fairly well described by a freely-expanding conical jet model with a single impulsive ejection event.

Alternatively, if the knot were to decelerate owing to interactions with the ISM, the release of energy would be expected to cause a brightening of the knot, as seen in both XTE J1550-564 (Corbel et al. 2002) and XTE J1748-288 (Hjellming et al. 1998). The low initial point could thus be due to a slight rebrightening between 4 and 8 days after the outburst (i.e. within 135 mas of the core), but with only a single point, this remains highly speculative. There is no evidence for any significant rebrightening between 8 and 45 days after ejection, which would argue against deceleration during that time period. This is consistent with a picture in which the jet was initially confined by a dense medium close to the source, with which it interacted. Once the angular separation was sufficiently great, the lower density would cause the transition from slowed to free expansion, and in the absence of sufficient material to cause deceleration, the knot then moved outwards ballistically. However, with such

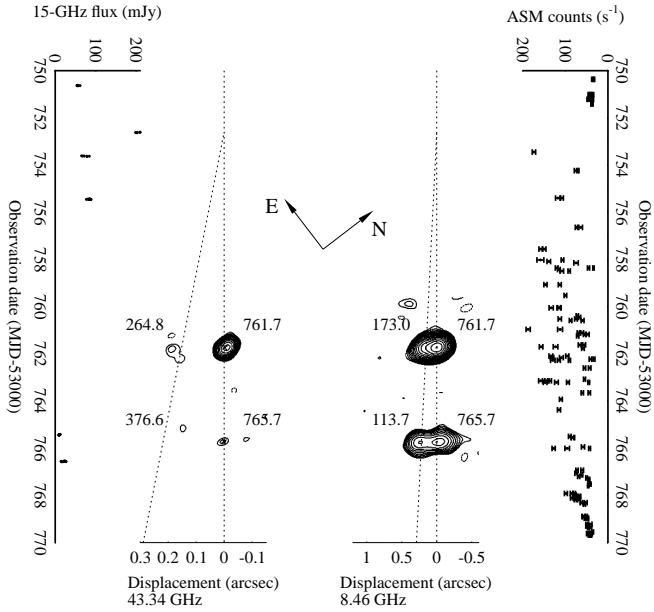


Figure 3. VLA images of the 2006 January ejection event. Flux densities from the 15-GHz Ryle monitoring programme are shown on the left-hand axis and the 1.5–12 keV X-ray count rates measured by the *RXTE* ASM are on the right-hand axis. The 43.34 GHz data are shown in the left-hand column of images, and 8.46 GHz images in the right-hand column. The dates of the observations are shown at the top right of each radio image, and the image rms (in $\mu\text{Jy bm}^{-1}$) at the top left. Contours are at levels of $\pm(\sqrt{2})^n$ times the rms level, where $n = 3, 4, 5, \dots$. The predicted position of the VLBA core (V. Dhawan, private communication) is marked by a cross. All images have been rotated clockwise by 52.5° . Dotted lines show the core position and a nominal proper motion of 17.0 mas d^{-1} for a knot ejected at the time of the Ryle flare.

sparse sampling of the early phase of the outburst, this scenario cannot be confirmed with the available data.

2.4 Combining the data

There is only one epoch of VLBA data (MJD 53794) in which the approaching component seen with the VLA was resolved. Subsequently, it is to be assumed that the knot had moved too far from the core, and expanded and faded too much to be detectable with the VLBA. For that one set of overlapping data, the two arrays detected the component at almost identical positions, and the VLBA saw only a single component, as opposed to a string of successive ejecta. This would suggest that it is unlikely that resolution effects between the different arrays are causing the measurement of different proper motions. MERLIN did not at any stage detect the original ejecta, but the first epoch of MERLIN data is later still, MJD 53797.

It is also not possible to track any of the VLBA knots between VLBA epochs, so we cannot definitively assign a proper motion to any of these knots. We strongly encourage future high-resolution observations to begin observing the source as quickly as possible after a flare, in order to be able to track the knots before they fade.

Nevertheless, we can use the start of the flare detected

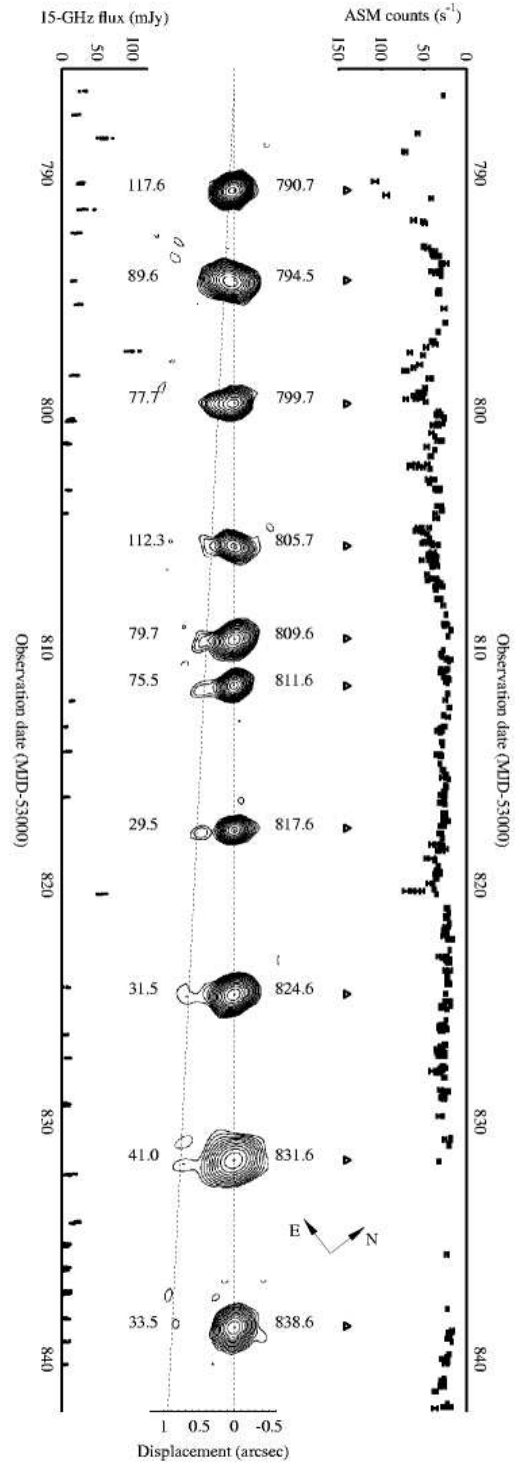


Figure 4. VLA images of the 2006 February ejection event (all at 8.46 GHz except for the 4.86 GHz image of MJD 53831.6). Flux densities from the 15-GHz Ryle monitoring programme are shown on the left-hand axis and the 1.5–12 keV X-ray count rates from the *RXTE* ASM are on the right-hand axis. Triangles in the X-ray plot mark the exact observation dates. The dates of the observations are shown to the right of each image, and the image rms (in $\mu\text{Jy bm}^{-1}$) to the left. Contours are at levels of $\pm(\sqrt{2})^n$ times the rms level, where $n = 3, 4, 5, \dots$. The predicted position of the VLBA core (V. Dhawan, private communication) is marked. All images have been rotated clockwise by 52.5° . Dotted lines show the core position and the fitted proper motion of 17.0 mas d^{-1} .

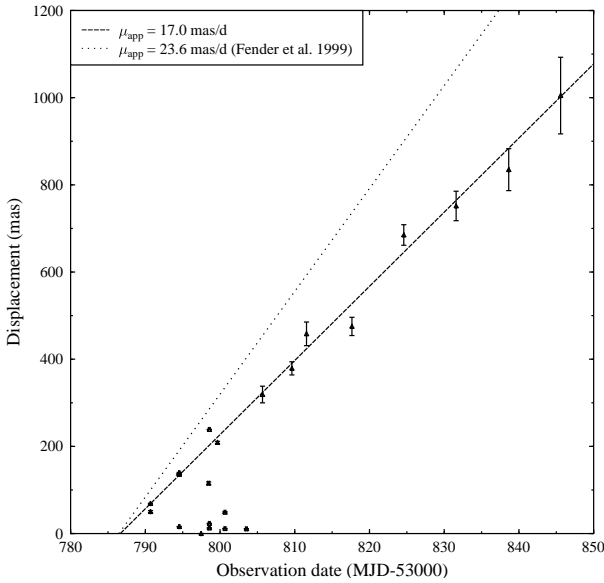


Figure 5. Measured angular separations from the core of the SE component ejected on MJD 53786. The separations measured with the VLBA and MERLIN are also included, which form the scatter of points at very low angular separations between MJD 53794 and 53803.

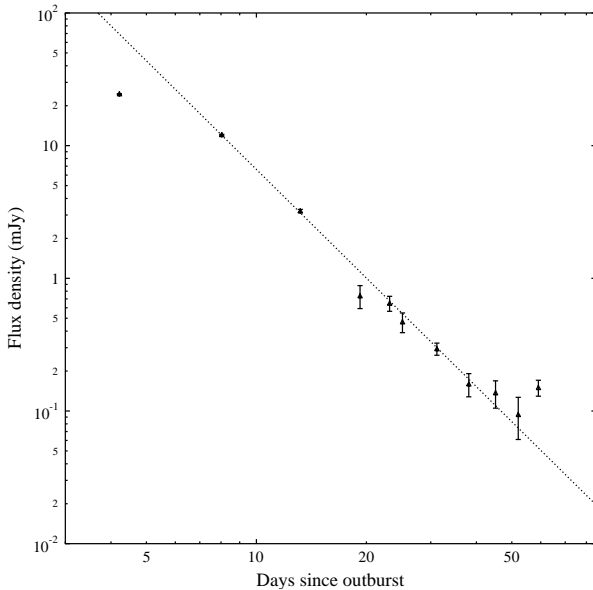


Figure 6. Measured VLA flux densities of the approaching jet knot ejected on MJD 53786, with a best-fitting line corresponding to a power-law decay of index 2.70 overlaid. Measurements at frequencies other than 8.4 GHz have had their flux densities scaled by an assumed spectral index $\alpha = -0.75$ ($S_\nu \propto \nu^\alpha$).

in the first epoch of MERLIN data to constrain the ejection event giving rise to the knots seen in the second epoch of VLBA data. If the outer pair of knots in the VLBA image are assumed to have been ejected at the time the flux density started to rise, it would imply proper motions of $21.1 \pm 0.3 \text{ mas d}^{-1}$ for the southeastern (approaching) knot and $11.7 \pm 0.3 \text{ mas d}^{-1}$ for the northwestern (receding) knot,

closer to what has previously been observed by the VLBA and MERLIN. But the start of the MERLIN flare is the latest possible time when the ejection event could have occurred. It is possible that the ejection happened earlier, moved outwards, and only caused an increase in the total flux density once it reached a point at which the knot became optically thin at the observing frequency. Thus these observations do not conclusively rule out an earlier ejection date and consequently a lower proper motion.

2.4.1 The receding component

The receding component was in no case unambiguously detected in our data from the 2006 February outburst, although there are hints of a receding component in the image of MJD 53817. We note that during previous ejection events, the receding component has not always been detected. Rodríguez & Mirabel (1999) observed the receding component in four of their five reported events, Fender et al. (1999) detected it in one of their three events, and Miller-Jones et al. (2005) in two of their four events. We assume that the outburst was not sufficiently bright to detect the Doppler-deboosted receding component once it was significantly far out to be resolved from the core.

The first epoch of VLBA data shows evidence for ejecta at a position angle consistent with being the receding northwestern component (see Table 2). The 2.3 GHz flux density peak is significantly closer to the core than that at 8.4 GHz, possibly suggesting that there were higher-energy particles present at the leading edge of the ejecta, consistent with the internal shock interpretation. Receding components are also seen at much smaller angular separations in the second epoch. We can use the angular separations from the core of corresponding approaching and receding knots to constrain the value of $\beta \cos \theta$ for those particular ejections, via

$$\beta \cos \theta = \frac{\mu_{\text{app}} - \mu_{\text{rec}}}{\mu_{\text{app}} + \mu_{\text{rec}}}, \quad (2)$$

where the time dependence of μ cancels out since we see all components in a single image. Applying this approach to the images of the first epoch (MJD 53794.5), this gives $\beta \cos \theta = 0.33 \pm 0.01$ at 8.4 GHz and 0.46 ± 0.02 at 2.3 GHz, close to the previous estimates of 0.323 ± 0.011 (Mirabel & Rodríguez 1994) and 0.41 ± 0.02 (Fender et al. 1999). Assuming that the two bright northwestern (receding) components seen in the second epoch of VLBA data (MJD 53798.6) correspond to the two bright approaching components, we find $\beta \cos \theta = 0.27 \pm 0.01$ for the furthest out pair (SE2 and NW2 in Table 2) and 0.22 ± 0.03 for the other pair (SE1 and NW1). In both cases this is significantly smaller than the values found in the literature, suggesting a possible misidentification of corresponding components or of the true core location.

If, as suggested in Section 2.3.3, the jet is freely expanding, then observational constraints on the opening angle and the derived value of $\beta \cos \theta$ can be used to place a lower limit on the Lorentz factor of the jet knot, as shown by Miller-Jones, Fender & Nakar (2006). The last 8.4-GHz VLA observation (MJD 53838.6) gives us the best constraints on the opening angle of the (unresolved) jet knot, $\phi < 19.6^\circ$. Together with the constraint on $\beta \cos \theta$ from the first set of 8.4-GHz VLBA images (Section 2.4.1), this allows us to derive a lower limit to the bulk Lorentz factor for any given

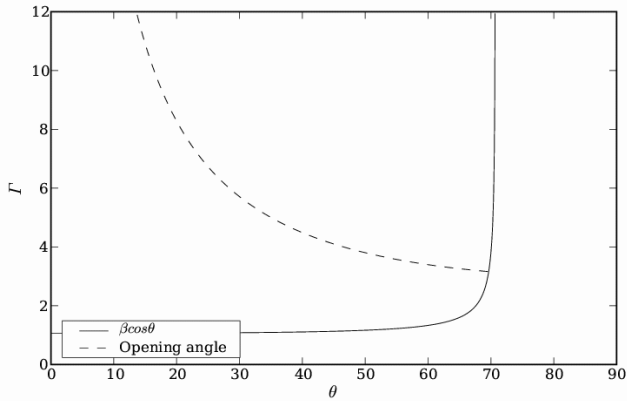


Figure 7. Variation of the derived Lorentz factor for the approaching jet knot with inclination angle to the line of sight. *Dotted line:* Minimum possible Lorentz factor derived from the measured upper limit on the jet opening angle, assuming free expansion. *Solid line:* Bulk Lorentz factor derived from the measured value of $\beta \cos \theta$ from the first epoch of VLBA observations.

value of the inclination angle, via

$$\Gamma = \left(1 + \frac{\beta_{\text{exp}}^2}{\tan^2 \phi \sin^2 \theta} \right)^{1/2}, \quad (3)$$

where $\beta_{\text{exp}}c$ is the jet knot expansion speed. The derived Lorentz factors for free expansion ($\beta_{\text{exp}} = 1$) are shown in Fig. 7. This suggests that the Lorentz factor should be > 3.2 during the freely-expanding phase. In order to agree with the constraint from the observed value of $\beta \cos \theta$, the source must be close to d_{max} (the maximum distance allowed by the measured proper motions of the radio jets, defined as $c/\sqrt{\mu_{\text{app}}\mu_{\text{rec}}}$). Such a Lorentz factor would agree with those derived by Fender et al. (1999) from MERLIN observations, assuming a distance close to $d_{\text{max}} = 11.2$ kpc.

2.4.2 Convolutions

For the few epochs when we have overlapping observations with different arrays, it is possible to convolve the higher resolution data to the resolution of the more compact array in order to check for consistency. Convoluting the VLBA data to the VLA resolution on MJD 53794.5, the resulting source morphology was found to be very similar. While not altogether unexpected, since the VLBA had detected a single extended component at the same position as the VLA detection, this is reassuring. Convoluting the VLBA data to the MERLIN resolution on MJD 53798.6, there was no evidence in the VLBA data at either frequency for the approaching component seen with MERLIN. This would tend to suggest that the component seen in the MERLIN data was relatively diffuse, since the largest angular scale probed by the VLBA is 41 mas at 8.4 GHz and 147 mas at 2.3 GHz, whereas MERLIN probed angular scales in the range 47 mas to 1.88 arcsec. This effect could also have prevented the high-resolution arrays from seeing the original ejected component after MJD 53794; once it had expanded sufficiently such that there was no structure on scales small enough to be seen with the high resolution arrays, it could not be detected. Coupled with the greater sensitivity of the VLA, this explains the

non-detection of the original southeastern component in the last three VLBA epochs and the last MERLIN epoch.

An attempt was also made to convolve the VLBA data taken on MJD 53798.6 and 53800.7 to the VLA resolution on MJD 53799.7. Since the observed VLBA structure was fairly small-scale and compact, there was no detection of the extension seen in the VLA image. The proper motion discrepancy cannot therefore be definitively ascribed to the spatial averaging of underlying compact structures with the VLA. Hjellming & Rupen (1995) pointed out that a combination of the flux density of the ejecta fading with time and beam smearing effects could lead to inaccurate proper motion estimates. While this cannot be ruled out with the present data, the images of MJD 53794 suggest that this effect is not occurring in the current datasets, since only a single set of VLBA ejecta was observed, rather than a continuous string of knots.

3 DISCUSSION

The fact that we have measured the same proper motion (to within errors) as seen with the VLA in 1994 suggests that there has been no lasting fundamental change in the system since that time. This would seem to rule out the secular change scenario postulated by Miller-Jones et al. (2005) to explain the proper motion discrepancy. If, as suggested, the radio jets had only switched on in 1992, since when they had evacuated a cavity in the interstellar medium (ISM) allowing the jets to propagate further at high velocity before decelerating, then a high proper motion, of order 23.6 mas d^{-1} , should also be measured with our VLA data, which was not the case.

The VLBA data would suggest that resolution effects are not responsible for the discrepancy between the proper motions measured on large and small angular scales. As well as the range of angular scales probed by MERLIN and the VLA overlapping, the image of MJD 53794 shows only a single VLBA component, rather than a string of successive knots. The convolutions presented in Section 2.4.2 further argue against this possibility.

From the range of proper motions that we have measured, and from the values quoted in the literature (Table 1), it would appear that GRS 1915+105 is capable of producing ejecta with a range of proper motions. In no case has there ever been any evidence for deceleration. Thus, if the spread of proper motions is intrinsic, this would imply that the speeds of the jet knots are not fixed by the properties of the black hole powering the jets (its mass, spin or magnetic field). The variation in the speed of the ejecta is in fact a feature of the so-called “unified model” of black hole X-ray binaries proposed by Fender, Belloni & Gallo (2004), whereby the Lorentz factor of the jets increases as the X-ray spectrum softens in the Very High State, leading to internal shocks within the flow which are seen as discrete ejecta. For those discrete ejecta to have different observed proper motions would then imply a variable velocity discrepancy between the jet Lorentz factor in the hard and quiescent states, and that in the soft state. Since the inner edge of the accretion disc is believed to move inwards during this transition between the hard and soft states, this would imply a different inner disc radius for each outburst. This is cer-

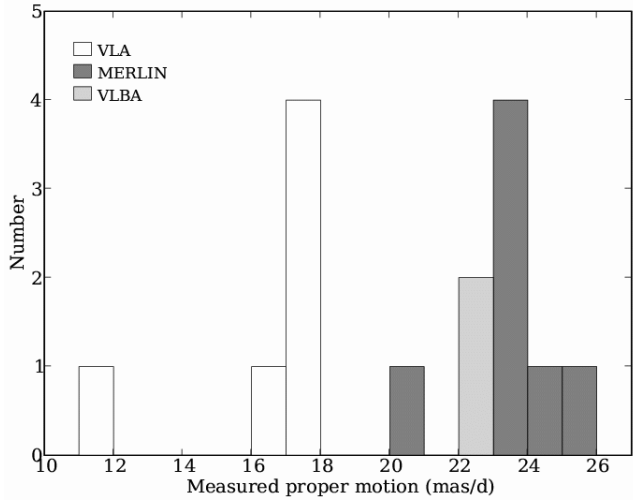


Figure 8. Histogram of the measured proper motions of the approaching jet knot of GRS 1915+105, colour-coded by array. Data taken from Table 1. The measurement of $11 \pm 2 \text{ mas d}^{-1}$ is considered unreliable, since the jets were resolved in only one image.

tainly plausible, and would also explain the variable values of $\beta \cos \theta$ quoted in Section 2.4.1 and in the literature.

There is in fact no strong evidence for the jets in any X-ray binary to have identical proper motions during different outbursts. The number of systems in which radio proper motions from multiple outbursts have been measured is small (GRS 1915+105, Cygnus X-3, GRO J 1655-40, and SS 433). SS 433 has the most well-monitored and constant jet velocity of $\sim 0.26c$, but Blundell & Bowler (2005) have shown that the jet velocity does indeed vary, with a standard deviation of 0.013 in β . Thus while a varying proper motion in GRS 1915+105 would not necessarily go against the trend, it seems highly coincidental that if the observed speeds are drawn from some underlying distribution, there should be such a clear distinction between the high proper motions observed only by the high-resolution arrays, and the lower values seen only with the VLA (see Fig. 8). At present however, we are still in the regime of small number statistics. Nevertheless, applying a Kolmogorov-Smirnov test (e.g. Press et al. 1992) to see whether the VLA and higher-resolution observations could be drawn from the same distribution gives a probability of 3.63×10^{-4} (8.24×10^{-4} if the August 1995 point is ignored). This therefore seems unlikely.

Since we were unable to track the ejecta from the initial event with the VLBA and MERLIN, we cannot definitively rule out the possibility that the ejecta decelerated on angular scales $< 100 \text{ mas}$, before the VLA was able to accurately resolve them. In fact, extrapolating the proper motion measured with the VLA back to zero angular separation gives an ejection date of MJD 53786.65, 1.86 d prior to the peak of the 15-GHz radio flare detected with the Ryle Telescope. Although since, as previously noted, the radio flare is the latest possible date of ejection such that the true ejection date could have been somewhat earlier, this might be taken as suggestive of deceleration between the radio flare and the first set of VLA observations. Assuming an initial proper motion of 23.6 mas d^{-1} and an ejec-

tion date corresponding to the time of the 15-GHz radio flare, then extrapolating the best fitting line for the VLA proper motion backwards in time would imply that the deceleration would be occurring on angular scales of $\sim 70 \text{ mas}$ from the core. Previous MERLIN observations (Fender et al. 1999; Miller-Jones et al. 2005) have tracked the ejecta out to angular scales of $> 300 \text{ mas}$, with no compelling evidence for deceleration. Fig. 9 shows how the angular separations changed with time since ejection for all the events reported in the literature (using the derived ejection dates). From this figure, there is no clear evidence that deceleration occurs at any specific distance from the core. The diagram shows two clear tracks, one sampled by the higher-resolution arrays, and the other, with lower proper motions, by the VLA. The receding jet angular separations all appear to lie on the same track.

Circumstantial evidence for deceleration on small scales in GRS 1915+105 can be seen in the linear polarisation ‘rotator event’ observed in January 2001 by Fender et al. (2002). The electric vector position angles measured with the Australia Telescope Compact Array (ATCA) at 4.80 and 8.64 GHz rotated smoothly together through 50° over the course of $\sim 0.2 \text{ d}$. The constant separation between the position angles at the two frequencies ruled out Faraday rotation, and this was attributed to a changing magnetic field orientation. We note however that Blandford & Konigl (1979) suggested that an accelerating (or decelerating) jet would show a swing in polarisation position angle as the aberration angle varied. If this was the true explanation for the ‘rotator event’, and we attribute the detected polarisation to the southeastern (approaching) component (as seen by Fender et al. 1999; Miller-Jones et al. 2005), which we assume to have been ejected at the time of the spike in the *RXTE* data shown by Fender et al. (2002), then this deceleration would have been occurring somewhere between 0.2 and 1.0 d after ejection. Such an effect was not seen in the ATCA observations of the March 2001 ejection event, taken between 1.5 and 1.9 d after the zero-separation date derived by Miller-Jones et al. (2005). This would imply that if all outbursts followed the same pattern, deceleration would have to occur within $\sim 50 \text{ mas}$. Polarisation position angles measured by MERLIN (Fender et al. 1999; Miller-Jones et al. 2005) show large swings (albeit at a single frequency, such that Faraday rotation cannot be discounted) between 3 and 4 d after ejection, which would constrain the deceleration to occur within 70–100 mas. However, this evidence remains circumstantial, and would appear to be at odds with the MERLIN points 8–13 d after ejection on the 23.6 mas d^{-1} track in the inset to Fig. 9.

If the jets are indeed decelerating on angular scales of order 70 mas, then for a given source distance, we can find the change in β , and hence the change in the bulk Lorentz factor Γ and the amount of energy lost to the environment.

The proper motion of an approaching jet knot is given by

$$\mu_{\text{app}} = \frac{c\beta \sin \theta}{d(1 - \beta \cos \theta)}, \quad (4)$$

where β is the intrinsic jet speed, θ is the inclination angle of the jet axis to the line of sight, c is the speed of light, and d is the source distance. For a constant source distance, a changing proper motion requires either a change

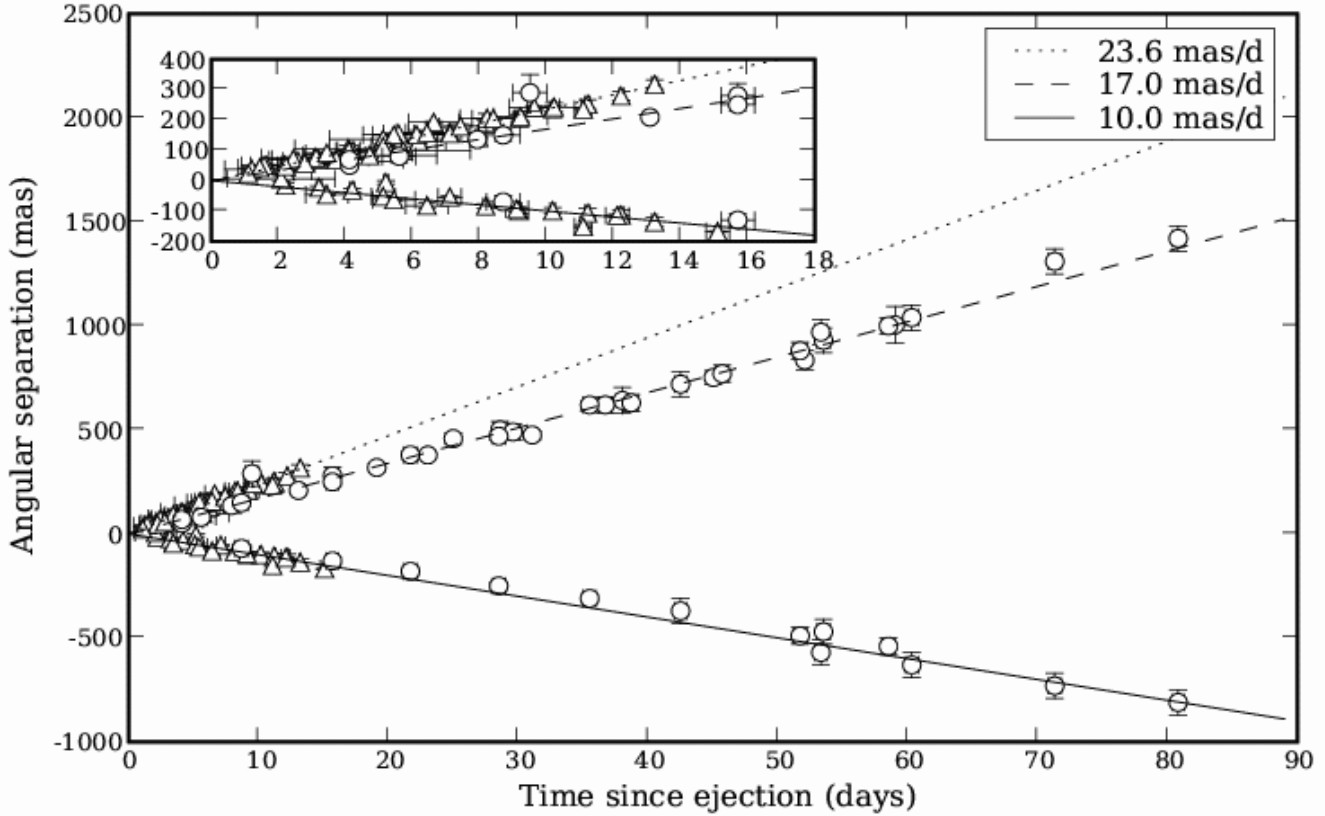


Figure 9. Variation in measured angular separation with time since ejection. Data taken from VLA (Rodríguez & Mirabel 1999, and Table 3), MERLIN (Fender et al. 1999; Miller-Jones et al. 2005) and VLBA (Dhawan et al. 2000, and Table 2) observations of GRS 1915+105. Ejection dates were taken from the ballistic proper motion fits reported in the source literature. Open circles show VLA data, open triangles show VLBA or MERLIN data. The inset shows a zoomed-in version of the smallest angular scales. There is no clear evidence for deceleration on any angular scale.

in β or a change in θ . The value of the product $\beta \cos \theta$ is constrained by measurements of the approaching and receding proper motions, via Equation 2. This was measured by Fender et al. (1999) to be $\beta \cos \theta = 0.41 \pm 0.02$ for the MERLIN-scale jets (with $\mu_{\text{app}} = 23.6 \pm 0.5 \text{ mas d}^{-1}$) and by Mirabel & Rodríguez (1994) to be $\beta \cos \theta = 0.323 \pm 0.011$ for the VLA-scale jets ($\mu_{\text{app}} = 17.6 \pm 0.4 \text{ mas d}^{-1}$). Combining Equations 2 and 4 gives a value for β ,

$$\beta = \sqrt{\frac{\mu_{\text{app}}^2 d^2 (1 - \beta \cos \theta)^2}{c^2} + (\beta \cos \theta)^2}, \quad (5)$$

taking $\beta \cos \theta$ to be a measured quantity. For a given distance, we can solve for the jet speed, β , and hence find the bulk Lorentz factor $\Gamma = (1 - \beta^2)^{-1/2}$.

Further, we can find the minimum energy associated with the synchrotron emission from the jet knots, given by (e.g. Longair 1994)

$$E_{\text{min}} = \frac{7}{6\mu_0} V^{3/7} \left(\frac{3\mu_0}{2} G(\alpha) \eta L_\nu \right)^{4/7}, \quad (6)$$

where V is the source volume, μ_0 is the permeability of free space, $(\eta - 1)$ is the ratio of the energy in protons to that in relativistic electrons, L_ν the source luminosity, and

$$G(\alpha) \propto \left(\nu_{\text{min}}^{\alpha+1/2} - \nu_{\text{max}}^{\alpha+1/2} \right) \nu_{\text{obs}}^{-\alpha}. \quad (7)$$

Assuming a spherical source of radius given by the light crossing time Δt , we can express $V = 4\pi(c\Delta t)^3/3$. The luminosity is $L_\nu = 4\pi d^2 S_\nu$, where S_ν is the source flux density. Factoring in the relevant constants of proportionality (assuming $\alpha = -0.75$; a different value would only change the numerical constant), we find that

$$E_{\text{min}}(\Gamma = 1) = 3.5 \times 10^{33} \eta^{4/7} \left(\frac{\Delta t}{\text{s}} \right)^{9/7} \left(\frac{d}{\text{kpc}} \right)^{8/7} \times \left(\frac{\nu}{\text{GHz}} \right)^{2/7} \left(\frac{S_\nu}{\text{mJy}} \right)^{4/7} \text{ erg}, \quad (8)$$

where the rise time of the flare Δt , the flux density S_ν , and the frequency ν at which the flare is observed should be measured in the source rest frame, equivalent to the observer's frame for $\Gamma = 1$. If the source is moving relativistically, then the transforms $\nu = \delta \nu'$, $S_\nu = \delta^{3-\alpha} S'_\nu$, and $\Delta t = \delta^{-1} \Delta t'$ must be applied, where δ is the Doppler factor $[\Gamma(1 - \beta \cos \theta)]^{-1}$. Care must be taken when transforming Equation 7, since the standard procedure is to set $\nu_{\text{max}} = \infty$ and $\nu_{\text{obs}} = \nu_{\text{min}}$. This should however be done after boosting, since the transformation of ν_{obs} is already accounted for by the extra factor α in the transformation of S_ν . Thus only ν_{min} should be relativistically boosted. Taking this into account, and multiplying the result by an extra factor Γ to account for the energy associated with the bulk motion of

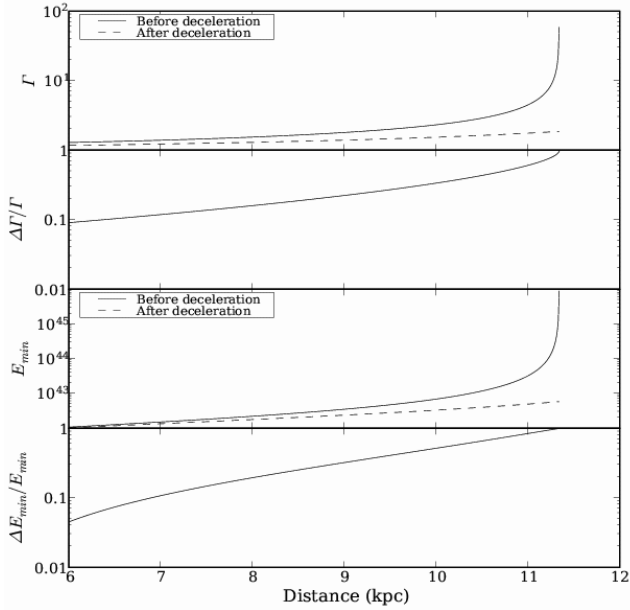


Figure 10. *Top panel:* variation with distance of Lorentz factor prior to deceleration ($\mu_{\text{app}} = 23.6 \pm 0.5 \text{ mas d}^{-1}$, $\beta \cos \theta = 0.41$) and after deceleration ($\mu_{\text{app}} = 17.6 \text{ mas d}^{-1}$, $\beta \cos \theta = 0.323$). *Second panel:* Fractional change in Lorentz factor during deceleration. *Third panel:* Minimum energy calculated before and after deceleration, using the Lorentz factors shown above. *Bottom panel:* Fractional change in minimum energy of the jet knots during deceleration.

the flow, the appropriate correction is then

$$E_{\text{min}}(\Gamma \neq 1) = \Gamma \delta^{-5/7} E_{\text{min}}(\Gamma = 1), \quad (9)$$

if the measured values in the observer’s frame are to be used. Taking the values quoted by Fender et al. (1999) of $\alpha = -0.8$, $\Delta t = 12 \text{ h}$, $\nu = 2.3 \text{ GHz}$ and $S_\nu = 550 \text{ mJy}$, together with $\eta = 1$, then for a given distance, calculating Γ (using $\beta \cos \theta = 0.41$ and $\mu_{\text{app}} = 23.6 \text{ mas d}^{-1}$) allows us to find the energy of the jet knots. Subsequently allowing a deceleration to $\beta \cos \theta = 0.323$ and $\mu_{\text{app}} = 17.6 \text{ mas d}^{-1}$ allows us to calculate the fractional energy loss from such a deceleration. The results of these calculations are shown in Fig. 10. If the source is decelerating, then if it lies close to d_{max} , it would lose almost all its energy in decelerating from 23.6 to 17.6 mas d^{-1} . Even at a distance of 6 kpc , its bulk Lorentz factor would decrease by 10 per cent and it would deposit 4 per cent of its energy into the surrounding ISM.

The only X-ray binaries in which conclusive evidence for deceleration has thus far been observed are XTE J1748-288 and XTE J1550-564. Four years after the initial ejection event of XTE J1550-564 in September 1998 (Hannikainen et al. 2001), the jets were seen to reappear at radio and X-ray wavelengths (Corbel et al. 2002) at angular separations of $\sim 23''$. Proper motions were obtained for the X-ray knots (Kaaret et al. 2003) which showed that the knots were decelerating, presumably due to some interaction with the surrounding ISM. Similar X-ray knots have also been detected in H 1743-322 (Corbel et al. 2005), and while deceleration has not been directly observed, it is possible that these knots were also powered by bulk deceleration. It was postulated that the jet knot from the 1998

outburst of XTE J1748-288 decelerated (Hjellming et al. 1998), although no definitive analysis is available in the literature. The knot was seen to stop at an angular separation of $\sim 300 \text{ mas}$ and brighten, almost as if it had hit a wall. Another case where there is possible evidence for deceleration is that of Cygnus X-3, where the milliarcsecond-scale structure shows a brighter, approaching southern jet (Mioduszewski et al. 2001; Miller-Jones et al. 2004) and a fainter receding northern counterjet, whereas the arcsecond-scale structure shows the northern jet knot to be brighter and at a larger angular separation from the core (Martí et al. 2001). This could also be interpreted as evidence for deceleration between these two sets of angular scales. Thus while deceleration has been directly observed on large angular scales, XTE J1748-288 and Cygnus X-3 are the only cases where this might be occurring so close to the centre of the system as required here in the case of GRS 1915+105. Cygnus X-3, while a very active radio emitter, has a Wolf-Rayet companion (van Kerkwijk et al. 1996) with a dense stellar wind, so its immediate environment would likely be denser than that surrounding GRS 1915+105, which has a K-M III companion (Greiner et al. 2001). There is also still speculation about the nature of the compact object in Cygnus X-3. Little is known about XTE J1748-288. Its compact object is very likely to be a black hole (Revnivtsev et al. 2000), but the nature of its companion is as yet unknown. However, in this system deceleration was clearly observed, with the jet knot appearing to stop and brighten, which is certainly not the case in GRS 1915+105.

Ultimately, the evidence for deceleration in GRS 1915+105 is not conclusive. It is perhaps most likely that the jet speed in this system is indeed variable, although the VLA and higher-resolution proper motion measurements do not appear to be drawn from the same distribution of speeds. More observations are certainly needed to verify this, since we are still in the regime of small number statistics.

4 CONCLUSIONS

We have measured the proper motion of a jet knot ejected during the 2006 February outburst of GRS 1915+105 as 17.0 mas d^{-1} . This is the first measurement of such a low proper motion since 1995, and shows that there has been no significant permanent change in the system which would allow the jet knots to propagate at a faster speed. The VLBA images have shown that although the first ejection was the brightest, there were in fact several ejection events over the course of two weeks after the radio outburst was first detected. The brightest jet knot shows no evidence for deceleration on angular scales greater than 100 mas , and its flux density decays as a simple power law between 8 and 45 days after the ejection event, with a power law index suggestive of a freely-expanding jet. In this case, the bulk Lorentz factor of the jet would be constrained to $\Gamma > 3$. By making simultaneous observations with multiple arrays probing different angular scales, we showed that the slower proper motions measured by the VLA are unlikely to be due to resolution effects.

Despite the aim of this set of observations being to cover a single outburst over a large range of angular scales using

the VLBA, MERLIN and the VLA, the high-resolution observations could not be triggered early enough to properly track the knots seen with the VLA, and we were unable to conclusively resolve the discrepancy in the proper motions. In order to find out what is really going on, it will be important to begin observing within one or two days of the detection of the outburst with the VLBA and MERLIN, to track the knots on the smallest angular scales while they are still bright, and to attempt to follow the same knots with the A-configuration VLA as they move outwards. Following a brighter outburst would also help, enabling monitoring with higher positional accuracy and out to larger angular distances (particularly important for the high-resolution arrays). If, as suggested by Truss & Done (2006), the accretion disc in GRS 1915+105 is now almost empty, then the source may soon switch off. There may therefore be few opportunities left to initiate such a monitoring programme, since it requires a bright outburst to occur while the VLA is in its A configuration.

ACKNOWLEDGMENTS

The National Radio Astronomy Observatory is a facility of the National Science Foundation operated under cooperative agreement by Associated Universities, Inc. The X-ray data presented are quick-look results provided by the ASM/*RXTE* team. MERLIN is operated as a National Facility by the University of Manchester at Jodrell Bank Observatory on behalf of the Particle Physics and Astronomy Research Council (PPARC). JCAM-J would like to thank Sebastian Jester for useful discussions and the anonymous referee for their constructive feedback.

REFERENCES

- Blandford R. D., Konigl A., 1979, *ApJ*, 232, 34
 Blundell K. M., Bowler M. G., 2005, *ApJ*, 622, L129
 Castro-Tirado A. J., Brandt S., Lund N., 1992, *IAU Circular*, 5590, 2
 Corbel S., Fender R. P., Tzioumis A. K., Tomsick J. A., Orosz J. A., Miller J. M., Wijnands R., Kaaret P., 2002, *Science*, 298, 196
 Corbel S., Kaaret P., Fender R. P., Tzioumis A. K., Tomsick J. A., Orosz J. A., 2005, *ApJ*, 632, 504
 Dhawan V., Mirabel I. F., Rodríguez L. F., 2000, *ApJ*, 543, 373
 Fender R. P., Garrington S. T., McKay D. J., Muxlow T. W. B., Pooley G. G., Spencer R. E., Stirling A. M., Waltman E. B., 1999, *MNRAS*, 304, 865
 Fender R. P., Rayner D., McCormick D. G., Muxlow T. W. B., Pooley G. G., Sault R. J., Spencer R. E., 2002, *MNRAS*, 336, 39
 Fender R. P., Belloni T. M., Gallo E., 2004, *MNRAS*, 355, 1105
 Greiner J., Cuby J. G., McCaughrean M. J., Castro-Tirado A. J., Mennickent R. E., 2001, *A&A*, 373, L37
 Hannikainen D., Campbell-Wilson D., Hunstead R., McIntyre V., Lovell J., Reynolds J., Tzioumis T., Wu K., 2001, *Astrophysics and Space Science Supplement*, 276, 45
 Heinz S., 2002, *A&A*, 388, L40
 Hjellming R. M., Johnston K. J., 1988, *ApJ*, 328, 600
 Hjellming R. M., Rupen M. P., 1995, *Nature*, 375, 464
 Hjellming R. M., Rupen M. P., Mioduszewski A. J., Smith D. A., Harmon B. A., Waltman E. B., Ghigo F. D., Pooley G. G., 1998, *Bulletin of the American Astronomical Society*, 30, 1405
 Kaaret P., Corbel S., Tomsick J. A., Fender R., Miller J. M., Orosz J. A., Tzioumis A. K., Wijnands R., 2003, *ApJ*, 582, 945
 Kaiser C. R., Gunn K. F., Brocksopp C., Sokolowski J. L., 2004, *ApJ*, 612, 332
 Longair M. S., 1994, *High energy astrophysics. Vol.2: Stars, the galaxy and the interstellar medium*. Cambridge: Cambridge University Press, 2nd ed.
 Martí, J., Paredes, J.M., & Peracaula, M. 2001, *A&A*, 375, 476
 Mioduszewski A. J., Rupen M. P., Hjellming R. M., Pooley G. G., Waltman E. B., 2001, *ApJ*, 553, 766
 Miller-Jones J. C. A., Blundell K. M., Rupen M. P., Mioduszewski A. J., Duffy P., Beasley A. J., 2004, *ApJ*, 600, 368
 Miller-Jones J. C. A., McCormick D. G., Fender R. P., Spencer R. E., Muxlow T. W. B., Pooley G. G., 2005, *MNRAS*, 363, 867
 Miller-Jones J. C. A., Fender R. P., Nakar E., 2006, *MNRAS*, 367, 1432
 Miller-Jones J. C. A., Rupen M. P., Trushkin S. A., Pooley G. G., Fender R. P., 2006, *ATel* 758
 Mirabel I. F., Rodríguez L. F., 1994, *Nature*, 371, 46
 Pfenniger D., Revaz Y., 2005, *A&A*, 431, 511
 Pooley G. G., Fender R. P., 1997, *MNRAS*, 292, 925
 Press, W.H., Teukolsky, S.A., Vetterling, W.T., & Flannery, B.P. 1992, *Numerical Recipes in C: The Art of Scientific Computing* (Ed. 2; Cambridge: Cambridge University Press)
 Revnivtsev M. G., Trudolyubov S. P., Borozdin K. N., 2000, *MNRAS*, 312, 151
 Rodríguez L. F., Mirabel I. F., 1998, *A&A*, 340, L47
 Rodríguez L. F., Mirabel I. F., 1999, *ApJ*, 511, 398
 Truss M., Done C., 2006, *MNRAS*, 368, L25
 van Kerkwijk M. H., Geballe T. R., King D. L., van der Klis M., van Paradijs J., 1996, *A&A*, 314, 521